REGULAR ARTICLE

blood advances

Altered platelet-megakaryocyte endocytosis and trafficking of albumin and fibrinogen in *RUNX1* haplodeficiency

Fabiola Del Carpio-Cano,[1,*] Guangfen Mao,[1,*] Lawrence E. Goldfinger,[2,*] Jeremy Wurtzel,[2] Liying Guan,[1] Mohammad Afaque Alam,[1] Kiwon Lee,[3,4] Mortimer Poncz,[3] and A. Koneti Rao[1,5]

[1]Sol Sherry Thrombosis Research Center, Lewis Katz School of Medicine at Temple University, Philadelphia, PA; [2]Division of Hematology, Department of Medicine, Cardeza Foundation for Hematologic Research, Sidney Kimmel Medical College, Thomas Jefferson University, Philadelphia, PA; [3]Department of Pediatrics, Children's Hospital of Philadelphia, Philadelphia, PA; [4]Department of Bioscience and Biotechnology, Hankuk University of Foreign Studies, Seoul, Korea; and [5]Department of Medicine, Lewis Katz School of Medicine at Temple University, Philadelphia, PA

Key Points

- Platelet endocytosis of α-granule proteins, albumin, fibrinogen, and IgG were decreased in 2 patients with germ line RUNX1 haplodeficiency.
- In *RUNX1*-deficient HEL cells and MK, endocytosis was enhanced with defective trafficking leading to decreased protein levels.

Platelet α-granules have numerous proteins, some synthesized by megakaryocytes (MK) and others not synthesized but incorporated by endocytosis, an incompletely understood process in platelets/MK. Germ line *RUNX1* haplodeficiency, referred to as familial platelet defect with predisposition to myeloid malignancies (FPDMMs), is associated with thrombocytopenia, platelet dysfunction, and granule deficiencies. In previous studies, we found that platelet albumin, fibrinogen, and immunoglobulin G (IgG) were decreased in a patient with FPDMM. We now show that platelet endocytosis of fluorescent-labeled albumin, fibrinogen, and IgG is decreased in the patient and his daughter with FPDMM. In megakaryocytic human erythroleukemia (HEL) cells, small interfering RNA *RUNX1* knockdown (KD) increased uptake of these proteins over 24 hours compared with control cells, with increases in caveolin-1 and flotillin-1 (2 independent regulators of clathrin-independent endocytosis), LAMP2 (a lysosomal marker), RAB11 (a marker of recycling endosomes), and IFITM3. Caveolin-1 downregulation in RUNX1-deficient HEL cells abrogated the increased uptake of albumin, but not fibrinogen. Albumin, but not fibrinogen, partially colocalized with caveolin-1. *RUNX1* KD resulted in increased colocalization of albumin with flotillin and fibrinogen with RAB11, suggesting altered trafficking of both proteins. The increased uptake of albumin and fibrinogen, as well as levels of caveolin-1, flotillin-1, LAMP2, and IFITM3, were recapitulated by short hairpin RNA *RUNX1* KD in $CD34^+$-derived MK. To our knowledge, these studies provide first evidence that platelet endocytosis of albumin and fibrinogen is impaired in some patients with *RUNX1*-haplodeficiency and suggest that megakaryocytes have enhanced endocytosis with defective trafficking, leading to loss of these proteins by distinct mechanisms. This study provides new insights into mechanisms governing endocytosis and α-granule deficiencies in *RUNX1*-haplodeficiency.

Introduction

Endocytosis is a major mechanism by which cells, including platelets and megakaryocytes (MK), take up diverse molecules to traffic them to distinct intracellular membrane compartments.[1-5] Platelet

Submitted 30 June 2023; accepted 29 January 2024; prepublished online on *Blood Advances* First Edition 8 February 2024; final version published online 29 March 2024. https://doi.org/10.1182/bloodadvances.2023011098.

*F.D.C-C., G.M., and L.E.G. contributed equally to this study.

Data will be available upon request from the corresponding author, A. Koneti Rao (koneti@temple.edu).

The full-text version of this article contains a data supplement.

α-granules have numerous proteins; some, such as platelet factor (PF4) and von Willebrand factor (VWF), are synthesized by MK, whereas others, such as fibrinogen, albumin, immunoglobulin G (IgG), and factor V, are not synthesized by human MK but are incorporated into granules by endocytosis and endosomal trafficking.[1] In MK, after endocytosis, proteins sequentially traffic from early endosomes to multivesicular bodies to late endosomes, and finally to α-granules or to recycling endosomes for extrusion from the cell or to lysosomes for degradation.[6] Our understanding of mechanisms regulating endocytosis, trafficking, and granule formation in MK and platelets is incomplete.

Transcription factor RUNX1 is a major regulator of definitive hematopoiesis, megakaryopoiesis, and platelet production.[7-9] Human *RUNX1* haplodeficiency (RHD) owing to heterozygous germ line mutations is associated with familial thrombocytopenia, platelet dysfunction, α- and dense-granule deficiencies, and a predisposition to myeloid malignancies–a constellation termed familial platelet disorder with associated myeloid malignancy (FPDMM).[10-14] Platelet granules deficiencies are a hallmark of FPDMM,[11,14-16] but the underlying mechanisms are poorly understood.

In prior studies in a patient with FPDMM, we described the presence of α- and dense-granule deficiencies, and impaired activation-induced aggregation, secretion, protein phosphorylation (eg, pleckstrin and myosin light chain [MLC]), and αIIbβ3 activation.[11,16-19] On platelet expression profiling many genes were found to be downregulated,[18] and several were shown to be direct RUNX1 targets,[15,20-22] including *PF4*[21] and *MYL9*.[20] Our recent studies revealed that *RAB31*[23] and *RAB1B*[24]–2 small GTPases involved in endosomal trafficking (both *RUNX1* targets) are downregulated and associated with defective trafficking of VWF, mannose 6-phosphate receptor and epidermal growth factor receptor. An important finding in our patient was that platelets had decreased albumin, fibrinogen, and IgG[19]–proteins not synthesized by MK but incorporated by endocytosis.[1] To understand the mechanisms, we pursued the hypothesis that endocytosis and trafficking are impaired in platelets or MK in *RUNX1*-deficiency. Our studies provide the first evidence that FPDMM platelets have defective endocytosis of albumin, fibrinogen, and IgG. In *RUNX1*-deficient megakaryocytic human erythroleukemia (HEL) cells and MK differentiated from human $CD34^+$ cells, uptake of albumin and fibrinogen was increased with impaired trafficking by distinct mechanisms leading to decreased cellular levels. There was upregulation of caveolin-1 (Cav1) and flotillin-1 (Flot1), 2 proteins linked to clathrin-independent endocytosis,[4,25] and of lysosomal marker lysosome associated membrane protein 2 (LAMP2)[26] and recycling endosomal marker RAB11,[26,27] both linked to endosomal trafficking. These studies provide the first evidence that MK endocytosis and trafficking are perturbed in RHD.

Methods

Patient information

The patient is a previously described,[1-3] 40-year-old White male with FPDMM with a point mutation in *RUNX1* (*RUNX1* c.352-1 G>T) in intron 3 at the splice acceptor site for exon 4, leading to a frameshift with premature termination in the conserved Runt homology domain. We performed studies in his 17-year-old daughter, who has the same mutation. Healthy control participants were recruited from staff and students at the Lewis Katz School of Medicine at Temple University. This research was approved by institutional human subjects review board, and all participants gave a written informed consent.

Reagents

The following reagents were obtained: human fibronectin (EMD Millipore, Burlington, MA), poly-L-lysine solution (Sigma Life Science, St. Louis, MO), SPHERO Ultra Rainbow fluorescent particles (Spherotech, Inc, Lake Forest, IL), phorbol 12-myristate 13-acetate (PMA) (Enzo Life Sciences, Farmingdale, NY), human fibrinogen (Haematologic Technologies, Essex Junction, VT), and Pitstop 2 (Cayman Chemical, Ann Arbor, MI). Small interfering RNAs (siRNAs) against *RUNX1*, *CAV1*, *FLOT1*, *IFITM3* interferon induced transmembrane protein 3, and *CLTC* clathrin heavy chain, and control siRNAs, were purchased from Santa Cruz Biotechnology Inc, (Dallas, TX). Supplemental Table 1 presents the antibodies and other reagents used.

Preparation of platelets

Platelet-rich plasma was prepared by centrifugation (200 *g*, 20 minutes) from whole blood collected in 1 of 10 volume of 3.8% sodium citrate and incubated with carbacyclin (30 nM) for 20 minutes at room temperature (RT). Platelets were pelleted by centrifugation (650 *g*, 15 minutes, RT), resuspended in HEPES (4-(2-hydroxyethyl) piperazine-1-ethanesulfonic acid)-Tyrode buffer after washing twice by centrifugation (650 *g*, 10 minutes, RT) and used in experiments.

Studies in HEL cells

HEL cells obtained from the American Type Culture Collection (Rockville, MD) were cultured in RPMI 1640 medium (Cellgro, Manassas, VA), supplemented with 10% fetal bovine serum (FBS) (GE Healthcare, Mississauga, ON) and penicillin/streptomycin (100 U/mL per 100 mg/mL, Invitrogen) at 37°C in a humidified 5% CO_2 atmosphere. Cells were treated with 30 nM phorbol myristate acetate to induce megakaryocytic transformation.[28] PMA-treated HEL cells were transfected with 100 nM of *RUNX1*, *CAV1*, *FLOT1*, *IFITM3*, *CLTC*, or control siRNAs using Lipofectamine reagents (Invitrogen, Carlsbad, CA) and consisted of pools of 3 20 to 25 bp oligonucleotides (Santa Cruz Biotechnology, Dallas, TX). Cells were harvested at 24 to 48 hours after transfection and used for uptake studies.

Studies in primary MKs

Primary MK were grown in vitro from human $CD34^+$ hematopoietic stem cell progenitors as described and validated for studies on *RUNX1*-deficiency.[29,30] $CD34^+$ cells were infected with shRUNX1 or shNT-lentiviruses,[28,29] and cells expressing mCherry ($mCherry^+$) were sorted on day 4 and cultured until days 11 to 12 to obtain RUNX-deficient (shRX) and control (shNT) MK used for studies.

Protein uptake analyzed by flow cytometry

Protein uptake and retention (up to 24 hours) was studied in washed platelets, PMA-treated HEL cells and $CD34^+$ cell–derived MKs suspended in buffer using flow cytometry. Platelet suspensions (1×10^6/mL) were incubated with fluorescence conjugated Cy3-albumin (10 μg/mL), Cy3-fibrinogen (50 μg/mL), or Cy3-IgG (20 μg/mL) at 37°C for different times. HEL cells or MK (1.5×10^5) were incubated with fluorescent-conjugated albumin Alexa Fluor 488 (30 μg/mL), fibrinogen Alexa Fluor 647 (10 μg/mL), or

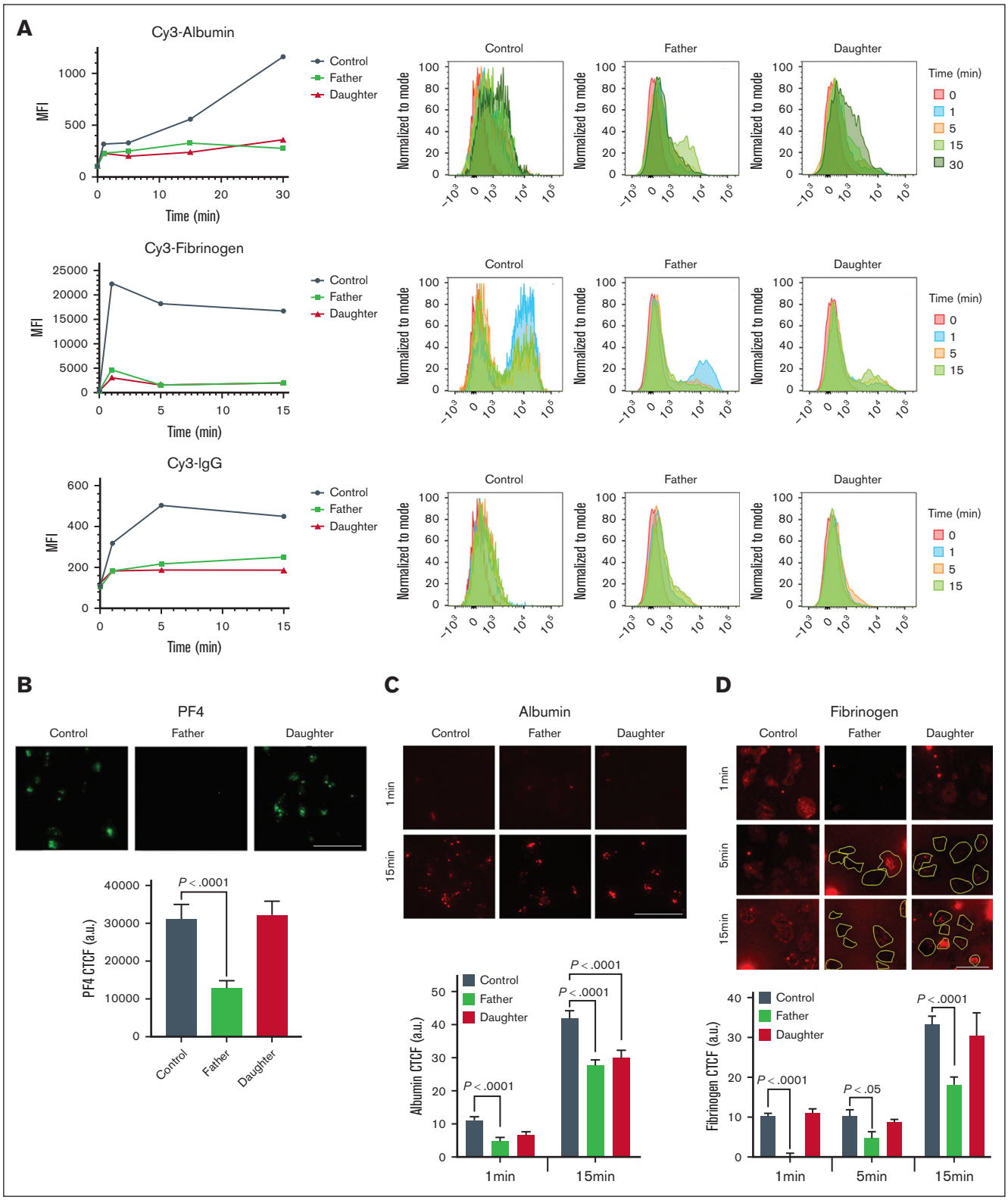

Figure 1. Studies on platelet uptake of albumin, fibrinogen and IgG in FPDMM. (A) Uptake of albumin, fibrinogen, and IgG by platelets from a father and daughter with FPDMM and a healthy control donor was assessed by flow cytometry. Washed platelets (1×10^6/mL) from all donors were incubated with Cy3-albumin (10 μg/mL), Cy3-fibrinogen (50 μg/mL), or Cy3-IgG (20 μg/mL) for 15 to 30 minutes at 37°C. Platelets were fixed and analyzed using flow cytometry and expressed as mean fluorescent intensity (MFI). (B) Immunofluorescence studies of platelet α-granule PF4 in patients with FPDMM. Platelets from the patients and the healthy control donor, immobilized on fibronectin-coated coverslips and fixed with 2% paraformaldehyde, were incubated with FITC-labeled anti-PF4 monoclonal antibody and images were taken using a Nikon E1000 microscope

IgG-Alexa Fluor 488 (30 μg/mL) at 37°C. Cells were fixed (2% paraformaldehyde) and uptake-retention was evaluated using a BD LSRII flow cytometry (San Jose, CA) and analyzed with FlowJo software, v10.5.3. The LSRII flow cytometer was calibrated using standard beads, SPHERO Ultra Rainbow Fluorescent Particles (Spherotech, Inc) on each experimental day. Where indicated, cells were incubated (15 minutes, RT) before uptake studies with 30 μM Pitstop 2 (Cayman Chemical).[4]

Protein uptake analyzed by immunofluorescence microscopy

Washed platelets (1.5 × 10^6/mL) were immobilized on coverslips precoated with 2 μg/mL human fibronectin (EMD Millipore, Rockville, MD) for 1 hour at 37°C; unbound platelets were removed by washing with HEPES Tyrode buffer (pH 7.4) and coverslips incubated with albumin Alexa Fluor 488, fibrinogen Alexa Fluor 647, or IgG-Alexa Fluor 488 (Jackson ImmunoResearch Lab, West Grove, PA) at 37°C for indicated times. Coverslips were rinsed with HEPES Tyrode buffer pH 7.4, fixed with 2% PFA for 15 minutes, and assessed using Epifluorescence microscope (EVOS FL Auto imaging). Anti-PF4 antibody was used to mark platelet α-granules.

HEL cells or MK were seeded on poly-L-lysine–coated coverslips and permeabilized with 0.1% Triton X-100 before immunostaining with antibodies as described.[16] The antibodies used are shown in supplemental Table 1. Images were obtained on an EVOS microscope or Leica TCS SP5 confocal microscope, using a 63×/1.40 n.a. oil immersion objective at RT and EVOS or Leica imaging software, respectively. Postacquisition processing and analysis were performed with Adobe Photoshop and ImageJ[31] and were limited to image cropping and brightness or contrast adjustments applied to all pixels per image simultaneously.

Studies on αIIBβ3 expression and activation and MLC phosphorylation

HEL cells (1 × 10^6/mL) treated with control or *RUNX1* siRNA were incubated with FITC (fluorescein isothiocyanate)-mouse antihuman CD41a clone–HIP8 or FITC-mouse antihuman PAC1 antibody (supplemental Table 1) to evaluate surface expression of αIIBβ3 complex in resting state and after activation with adenosine diphosphate (ADP; 50 μM) or thrombin (10 U/mL) (Millipore Sigma, Billerica, MA) using flow cytometry.

Immunoblotting of cell lysates

Cell lysates collected in M-Per protein extraction reagent (Pierce-Thermo Scientific) with protease inhibitors (Enzo Life Sciences) were subjected to 10% or 12% sodium dodecyl sulfate-polyacrylamide gel electrophoresis, transferred to 0.2 μM nitrocellulose membranes and probed with antibodies. Proteins were detected with IRDye-labeled secondary antibodies using Odyssey Infrared Imaging system (Li-Cor Biosciences).

Statistical analysis

Results were expressed as mean ± standard error of the mean. Differences were compared using Student *t* test or 1- and 2-way analysis of variance, using the GraphPad Prism, version 8 (GraphPad Software) and considered significant at $P < .05$.

Results

Platelet uptake of albumin, fibrinogen, and IgG is decreased in FPDMM

The uptake of Cy3-Chrom-albumin, Cy3-Chrom-fibrinogen, and Cy3-Chrom-IgG over 15 to 30 minutes was markedly decreased in platelets from the father and daughter with *FPDMM* compared with a healthy donor (Figure 1A). Because these proteins are incorporated into α-granules,[1] we assessed PF4 as an α-granule marker. It is synthesized by MK and is a RUNX1 target gene[21]; in prior studies, platelet PF4 protein and transcripts were decreased in the father.[18] PF4 immunofluorescence of cells immobilized on fibronectin was reduced in the father, consistent with α-granule deficiency, but not the daughter (Figure 1B). We studied albumin Alexa Fluor 488 and fibrinogen Alexa Fluor 647 uptake in platelets immobilized on fibronectin using immunofluorescence microscopy (Figure 1C-D). The uptake of albumin was decreased at 1 and 15 minutes in the father and daughter compared with the healthy donor (Figure 1C). At 1, 5, and 15 minutes the father's platelets had decreased fibrinogen; many platelets entirely lacked fibrinogen, whereas others had substantial uptake (Figure 1D), indicating heterogeneity among platelets. In the daughter the uptake appeared normal (Figure 1D). Overall, the uptake of albumin, fibrinogen, and IgG as analyzed by flow cytometry, was decreased in both patients; in the immobilized platelets, albumin uptake was decreased in both patients; whereas fibrinogen uptake was decreased in father but not in daughter, possibly because of differences in platelet adhesion between the 2 patients.

RUNX1 knockdown (KD) in HEL cells increases albumin uptake and upregulates Cav1 and Flot1

We assessed endocytosis in *RUNX1*-deficient HEL cells. In preliminary studies, the uptake of albumin Alexa 488 over 24 hours in PMA-treated HEL cells was concentration- (10-100 μg/mL) and time-dependent over 24 hours. With siRNA *RUNX1* KD, albumin uptake over 24 hours was increased compared with control cells

Figure 1 (continued) and quantified by ImageJ (v1.47; National Institutes Health). Corrected total cell immunofluorescence (CTCF) is shown (mean ± standard error of the mean [SEM]). *P* values shown are for comparisons by Student *t* test. (C) Albumin uptake in platelets from patients with FPDMM immobilized on fibronectin and assessed using immunofluorescence microscopy. Platelets from the father, daughter, and the healthy control donor, immobilized on fibronectin-coated coverslips, incubated with albumin Alexa Fluor 488 (30 μg/mL) (red) for the indicated time at 37°C and fixed. Images were taken with Epifluorescence microscope (EVOS FL Autoimaging) to evaluate internalized albumin. The panel (below) shows the CTCF (mean ± SEM) of albumin uptake in platelets from the patients and a control donor. *P* values shown are for comparisons by Student *t* test. (D) Fibrinogen uptake in platelets from patients with FPDMM immobilized on fibronectin and assessed using immunofluorescence microscopy. Platelets from the father and daughter with FPDMM and the healthy control donor were immobilized on fibronectin-coated coverslips and incubated with fibrinogen Alexa 546 (50 μg/mL) (red) for the indicated time at 37°C. Images were analyzed as described above. Platelets are outlined in yellow. Many platelets from the father were devoid of fibrinogen with a population showing substantial uptake. Daughter's platelets appeared similar to control. The panel (below) shows changes in CTCF of fibrinogen uptake in platelets from FPDMM patients and control donor. *P* values are for comparisons made by the Student *t* test.

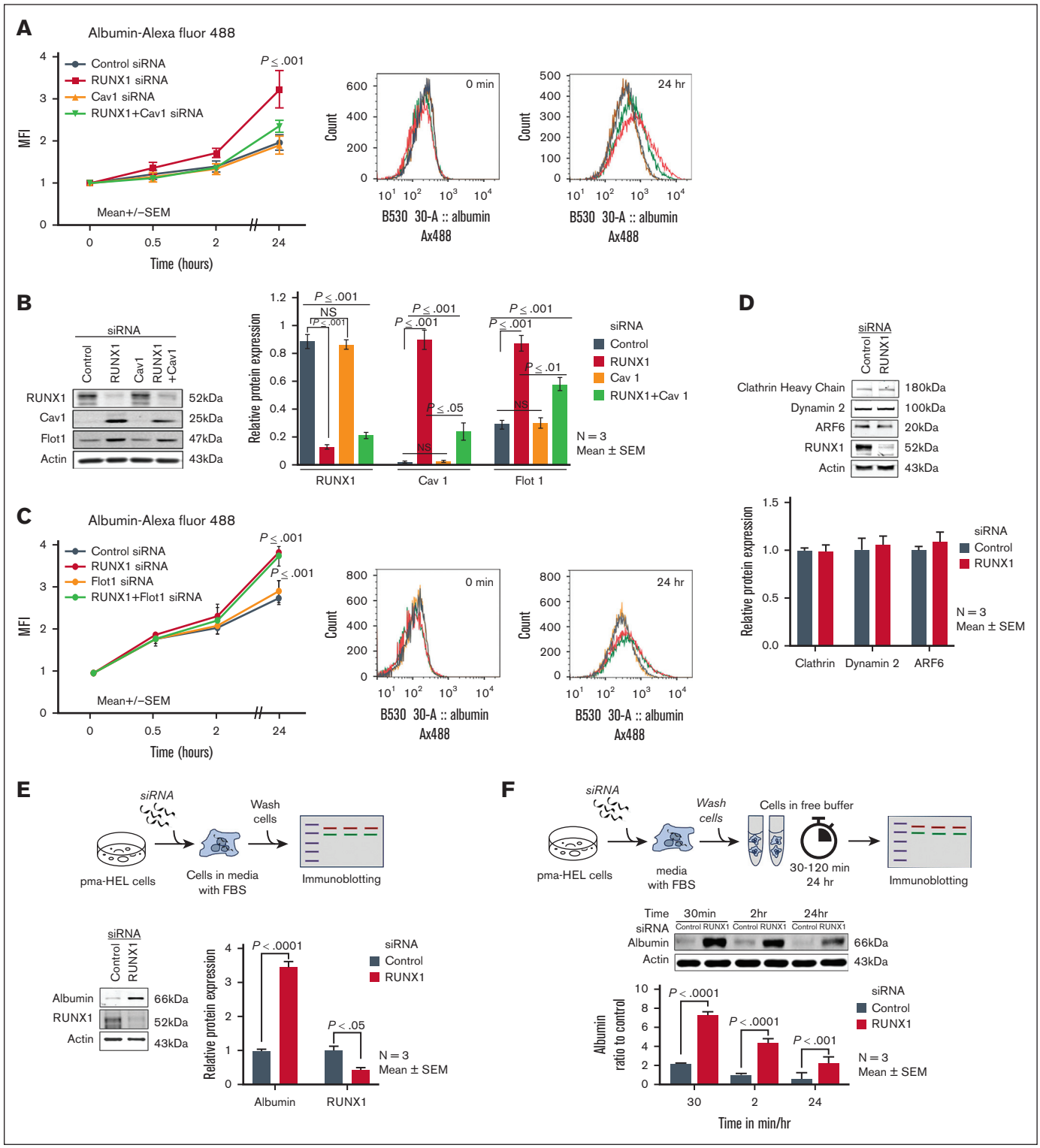

Figure 2. Effect of siRNA KD of *RUNX1*, *CAV1*, and *FLOT1* in HEL cells on uptake and retention of albumin. (A) Effect of siRNA KD of *RUNX1, CAV1,* and *RUNX1* + *CAV1* on uptake and retention of albumin was assessed by flow cytometry. PMA-treated HEL cells were transfected with siRNA oligos (100 nM) targeting *RUNX1*, *CAV1*, or combination of both for 48 hours. They were then incubated with 30 μg/mL albumin Alexa Fluor 488 for the indicated period, fixed, washed, and albumin uptake was assessed using flow cytometry. MFI is shown (mean ± SEM of 3 experiments). Control siRNA (black line); *RUNX1* siRNA (red); *CAV1* siRNA (orange); *RUNX1* + CAV1 siRNA (green). *P* values shown are for comparisons with control siRNA by Student *t* test. Representative flow cytometry histograms at 0 and 24 hours are shown on the right. (B) Immunoblots showing RUNX1, Cav1, and Flot1 with actin as loading control in control cells and after KD of RUNX1, *CAV1*, or both. The quantification is shown on the right (mean ± SEM, n = 3). *P* values are for comparisons by Student *t* test. (C) Effect of siRNA KD of *RUNX1*, *FLOT1*, or combination of both on uptake of albumin by flow cytometry. Following siRNA KD,

(Figure 2A). Cav1 and Flot1 are 2 major proteins involved in endocytosis.[2-5] Cav1 regulates albumin uptake in several cell types.[32,33] On immunoblotting, control HEL cells showed minimal Cav1, which increased markedly on *RUNX1* downregulation (Figure 2B). Although Flot1 was detected in control HEL cells, its expression increased further on *RUNX1* downregulation (Figure 2B). Notably, siRNA *CAV1* downregulation did not appear to decrease albumin uptake compared with control cells; however, it abrogated the increase in albumin uptake resulting from *RUNX1* KD (Figure 2A). *FLOT1* KD did not alter albumin uptake, and in contrast to the findings with *CAV1* downregulation, did not abrogate the increase in albumin uptake noted on *RUNX1* downregulation (Figure 2C). Immunoblotting confirmed the expected decreases in the respective proteins on KD of *RUNX1*, *CAV1*, and *FLOT1* and the increases in Cav1 and Flot1 on *RUNX1* downregulation (Figure 2B). *CAV1* downregulation did not affect Flot1 expression, and vice versa (not shown). Thus, *RUNX1* downregulation increased albumin uptake along with increased Cav1 and Flot1; the increased uptake was dependent on Cav1.

We examined other major proteins implicated in endocytosis. Clathrin-mediated endocytosis regulates fibrinogen uptake[1] and is dependent on dynamin-2,[3,5,34] and GTPase ARF6 (ADP ribosylation factor 6).[35] No changes were noted in these on *RUNX1* downregulation (Figure 2D).

In above experiments, HEL cells were cultured in an albumin-rich medium with FBS. We assessed albumin in washed HEL cells lysates after 24 to 48 hours of siRNA *RUNX1* KD. Albumin was increased upon *RUNX1* KD (Figure 2E). To assess the fate of endocytosed albumin, siRNA-treated HEL cells were resuspended in buffer without FBS, and levels assessed at 30 minutes, 2 hours and 24 hours in lysates. Albumin was higher in *RUNX1*-deficient cells at each time (Figure 2F). Under both conditions, the 24 hour albumin was lower than that at baseline, indicating loss over time, particularly in RUNX1-deficient cells.

RUNX1 KD increases fibrinogen uptake in HEL cells

In preliminary studies, HEL-cell fibrinogen uptake was dose- and time-dependent over 24 hours period. Fibrinogen Alexa Fluor 647 uptake over 24 hours was increased on *RUNX1* KD compared with control cells (Figure 3A). *CAV1* downregulation neither affected fibrinogen uptake in control cells nor the increased uptake on *RUNX1* downregulation (Figure 3A). *FLOT1* downregulation did not decrease uptake in control cells, but partially decreased it in *RUNX1*-deficient cells (Figure 3B). Thus, as with albumin (Figure 2), *RUNX1* KD increased fibrinogen uptake but was unaffected by *CAV1* KD.

To understand the fate of endocytosed fibrinogen, we assessed fibrinogen using immunoblotting in washed HEL cells after 24-hour incubation in media containing FBS and fibrinogen (50 μg/mL); the levels were lower in *RUNX1*-deficient cells compared with control cells (Figure 3C). In cells maintained in buffer over subsequent 24 hours, fibrinogen was lower in *RUNX1*-deficient cells at 30 minutes, 2 hours, and 24 hours (Figure 3D) indicating continued loss.

RUNX1 KD increases IgG uptake in HEL cells

Fluorescent-conjugated IgG uptake was increased in *RUNX1*-deficient compared with control cells (supplemental Figure 1).

Albumin colocalizes with Cav1, and this is lost with *RUNX1* KD and associated with increased colocalization with Flot1 and LAMP2

To understand the trafficking of albumin, we performed immunofluorescence microscopy of HEL cells, stained for Cav1, Flot1, and RAB11–a marker for recycling endosomes,[26,27] and LAMP2–a marker for lysosomes.[26] In control cells at 30 minutes, albumin colocalized with Cav1 but not with Flot1 (Figure 4A). Upon KD of *CAV1* alone or together with *RUNX1*, albumin was decreased indicating that *CAV1* regulates albumin uptake (Figure 4A). On *RUNX1* KD, there was loss of albumin colocalization with Cav1 and a strikingly increased colocalization with Flot1 (Figure 4A). There was no colocalization in the nuclear area (not shown). At 120 minutes, in the control cells, albumin colocalization with Cav1 was not as strong as observed at 30 minutes, and there was some albumin colocalization with Flot1 (Figure 4A). However, on *RUNX1* KD, there was little albumin colocalization with Cav1 and a strong colocalization with Flot1 (Figure 4A). With KD of *CAV1* alone or of *RUNX1* + *CAV1* there was no albumin in the cells. At 24 hours, albumin did not strongly colocalize with Cav1 or Flot1 in control or *RUNX1*-deficient cells (not shown). With respect to RAB11, immunoblots showed an increase on *RUNX1* KD (Figure 4B). However, at 30 and 120 minutes (Figure 4B) and at 24 hours (not shown), there was no albumin colocalization with RAB11 in control or *RUNX1*-deficient cells, suggesting that albumin does not traffic to recycling endosomes. In podocytes and other cells, albumin is degraded in lysosomes.[36,37] LAMP2 levels were increased on *RUNX1* KD on immunoblotting (Figure 4C). We observed moderate colocalization of albumin with LAMP2 at 30 minutes in control cells and on *RUNX1* KD (Figure 4C), but they did not appear to be different. At 120 minutes, the colocalization of albumin with LAMP2 appeared more prominent with *RUNX1* KD than in control cells (Figure 4C). Overall, these findings suggest RHD upregulates Cav1 and Flot1 (Figure 2), with altered albumin trafficking from Cav1 to Flot1 compartment, and increased colocalization with LAMP2 but not RAB11.

Figure 2 (continued) HEL cells were incubated with 30 μg/mL of albumin Alexa 488 for up to 24 hours, fixed, and analyzed by flow cytometry. Albumin uptake is expressed as MFI (mean ± SEM, n = 3). *P* values shown are for comparisons with control siRNA by Student t test. Control siRNA (black), *RUNX1* siRNA (red), *FLOT1* siRNA (orange), and *RUNX1* + *FLOT1* siRNA (green). Representative flow cytometry histograms are shown on the right. (D) Immunoblots showing relative levels of clathrin, dynamin-2, and ARF6 after *RUNX1* KD in HEL cells. The relative protein expression is shown below (n = 3). (E) HEL-cell albumin levels by immunoblotting after siRNA *RUNX1* KD. HEL cells were incubated with *RUNX1* siRNA for 24 hours in culture media containing fetal bovine serum. At 24 hours, the cells were washed with buffer and albumin levels assessed in cell lysates. Shown are a representative immunoblots with quantification of albumin and RUNX1 on the right (n = 3 experiments). (F) HEL-cell albumin levels over 24 hours in control cells and *RUNX1*-deficient cells. HEL cells were incubated with *RUNX1* or control siRNA for 24 hours in culture media containing FBS. At 24 hours, cells were washed and suspended in buffer without FBS. Albumin levels were assessed using immunoblotting in cell lysates at intervals shown. Shown is a representative immunoblot and quantification (n = 3 experiments).

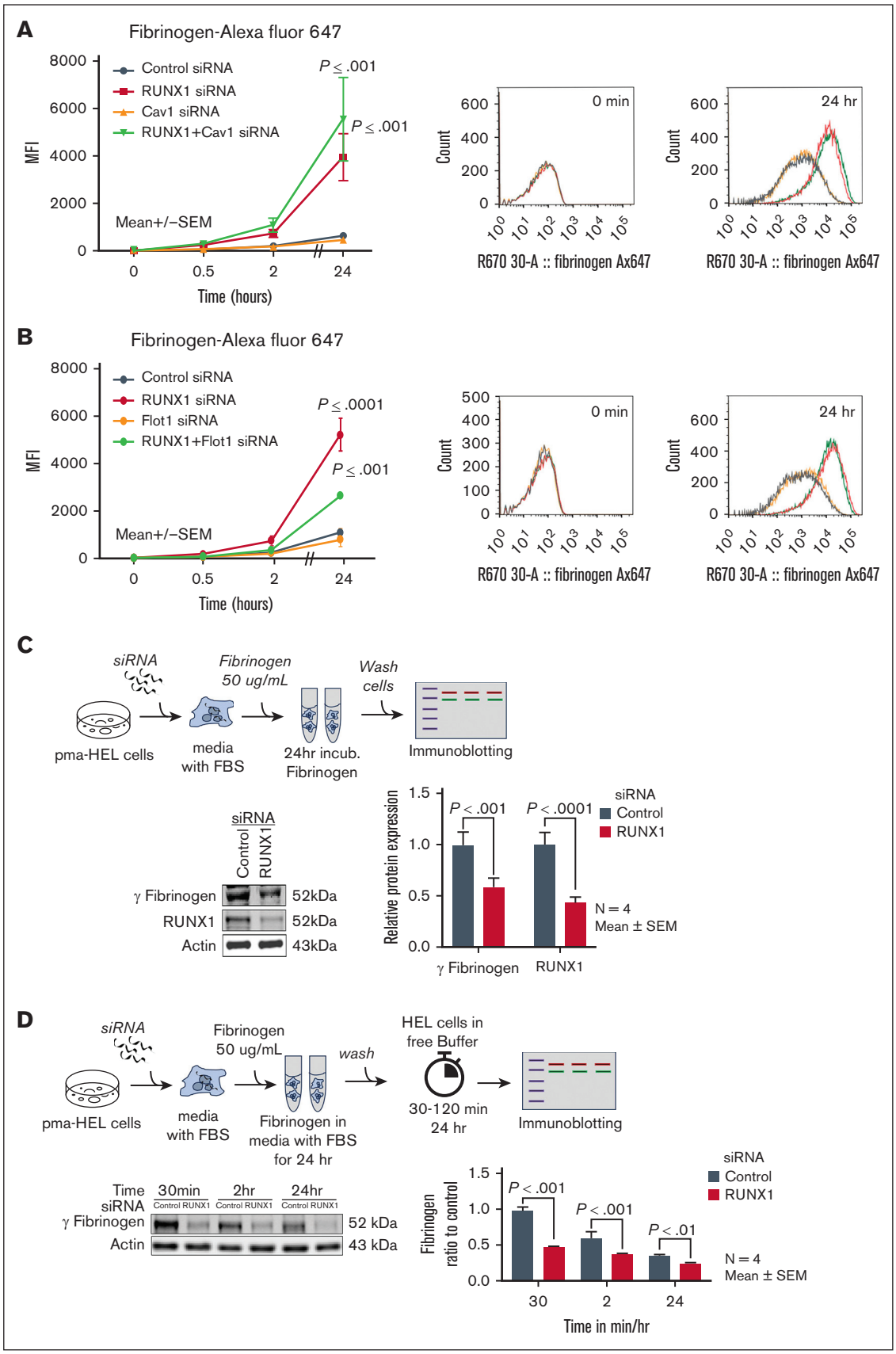

Figure 3.

Increased colocalization of fibrinogen with RAB11 on *RUNX1* KD

Fibrinogen uptake was unaffected by *CAV1* KD (Figure 5A), suggesting that it is not Cav1-dependent. In control cells or on *RUNX1* KD, we did not observe significant fibrinogen colocalization with Cav1 or Flot1 at 30 or 120 minutes (Figure 5A). Findings with respect to RAB11 were different. At 30 minutes, we observed low to moderate fibrinogen colocalization with RAB11 in control cells, which increased with *RUNX1* KD alone or together with *CAV1* (Figure 5B). However, colocalization with RAB11 was more prominent at 120 minutes (Figure 5B) and 24 hours (not shown). As noted earlier, RAB11 levels were increased with *RUNX1* downregulation (Figure 4B). These findings suggest that *RUNX1* KD causes trafficking of fibrinogen toward recycling endosomes. In both control cells and *RUNX1*-depleted cells, we observed moderate fibrinogen colocalization with LAMP2 at 30 minutes but was not different (Figure 5C).

RUNX1-deficient HEL cells recapitulate the defective αIIbβ3 activation and myosin phosphorylation in FPDMM platelets

MK fibrinogen uptake is αIIbβ3 receptor-mediated.[1,35,38,39] Our patient platelets have near normal surface αIIbβ3 expression but impaired agonist-induced activation (PAC binding) and MLC phosphorylation (pMLC),[17] the latter related to decreased expression of RUNX1-regulated gene *MYL9*.[18] Because fibrinogen uptake was increased on *RUNX1* KD (Figure 3), we assessed whether the HEL cells recapitulate these platelet abnormalities or show increased αIIbβ3. αIIbβ3 surface expression in *RUNX1*-deficient cells was comparable to that in control cells (Figure 6A); on immunoblotting αIIb was decreased with unchanged β3 (Figure 6B). Because surface αIIbβ3 drives fibrinogen uptake (Figure 6A), the impact of decreased cell lysate αIIb would be negligible. In HEL cells with *RUNX1* KD, thrombin and ADP-induced PAC1-binding (Figure 6C), total MLC protein and, correspondingly, thrombin-induced pMLC (Figure 6D) were decreased. Thus, *RUNX1*-deficient HEL cells recapitulate the platelet defects,[17-19] validating the HEL-cell model. When pMLC was expressed as a fraction of the total myosin, it was comparable between RHD HEL cells and control cells (Figure 6D), suggesting that phosphorylation mechanisms (MLC kinase-driven) were preserved. These studies indicate that increased fibrinogen uptake is not due to upregulated αIIbβ3 expression. Because αIIbβ3 activation is impaired in these cells (Figure 6C), it suggests that integrin activation is not a major driver of fibrinogen uptake.

Increased IFITM3 expression has been reported to enhance fibrinogen endocytosis in nonviral sepsis.[39] In HEL cells, it was increased on *RUNX1* KD (Figure 6E). However, *IFITM3* KD did not decrease fibrinogen uptake in control or *RUNX1*-deficient cells (supplemental Figure 2A). Fibrinogen uptake is clathrin-dependent,[1,39] and it was inhibited by clathrin inhibitor Pitstop 2 (supplemental Figure 2B).

RUNX1-deficient primary MKs recapitulate enhanced endocytosis

Albumin (Figure 7A) and fibrinogen (Figure 7B) uptake at 24 hours were increased in shRX compared with that in control shNT-MK, along with increased Cav1, Flot1, LAMP2, and IFITM3 (Figure 7C), whereas RAB11 was decreased (Figure 7C). On analysis with immunofluorescence microscopy, it was found that there was little albumin colocalization with Cav1 in shNT or shRX MK. In shRX *MK*, there was increased albumin colocalization with Flot1 (30 and 120 minutes) and LAMP2 at 30 minutes compared with shNT-MK (Figure 7D). There was minimal fibrinogen colocalization with RAB11 or LAMP2 in shNT-MK (supplemental Figure 3). In shRX MK, there was no increased fibrinogen colocalization with RAB11, as noted in HEL cells (Figure 4B). However, RAB11 was decreased in shRX MK (Figure 7C) in contrast with an increase in RUNX1-deficient HEL cells (Figure 4B). Fibrinogen colocalization with LAMP2 appeared minimally increased at 120 minutes in shRX MK (supplemental Figure 3). Further studies, beyond the scope of these studies, are needed to further delineate alterations in trafficking. The differences from the findings in HEL cells may reflect differences in cell maturity. Overall, shRX MK recapitulate the enhanced protein uptake, increases in Cav1, Flot1, LAMP2, and IFITM3 and increased albumin colocalization with Flot1 and LAMP2.

Platelet proteins in FPDMM

Compared with 3 healthy donors, Flot1, LAMP2, and RAB11 were not increased in FPDMM platelets (Figure 7E). Cav1 was undetectable in all donors, as reported.[34] IFITM3 was undetectable in the patient and 1 healthy donor. On platelet transcript profiling of our patient, these genes were not found among those increased.[18]

Discussion

Endocytosis is the mechanism by which proteins, not synthesized by MK, are incorporated into α-granules.[1] Platelet albumin, fibrinogen, and IgG were observed to be decreased in our patient[19] (and Figure 1). We provide the first evidence that platelet

Figure 3. Effect of siRNA KD of *RUNX1*, *CAV1*, and *FLOT1* on uptake and retention of fibrinogen in HEL cells. (A) Effect of siRNA KD of *RUNX1*, *CAV1*, or combination of both on uptake and retention of fibrinogen. PMA-treated HEL cells were transfected with siRNAs (100 nM): control (black dots), *RUNX1* (red), *CAV1* (orange), or combination of *RUNX1* + *CAV1* (green) for 48 hours. Cells suspensions were incubated with 10 μg/mL fibrinogen Alexa 647 for indicated times at 37°C, fixed and uptake was evaluated by flow cytometry. Shown mean ± SEM of 3 experiments. *P* values represent comparisons with control at 24 hours. Representative histograms are shown on the right. (B) Effect of siRNA KD of *RUNX1*, *FLOT1*, or combination of both on uptake and retention of fibrinogen by flow cytometry. *RUNX1* and *FLOT1* KDs were performed as described above. HEL cells were incubated with fibrinogen Alexa 647 (10 μg/mL) for indicated times. Data shown are mean of 2 experiments. Control cells (black), *RUNX1* KD (red), *FLOT1* KD alone (orange), combined *RUNX1*, and *FLOT1* KD (green). Representative histograms are shown on the right. (C) HEL-cell fibrinogen levels using immunoblotting after siRNA *RUNX1* KD. Cells treated with control and *RUNX1* siRNAs were washed and incubated in culture media containing fetal bovine serum and 50 μg/mL fibrinogen for 24 hours. Fibrinogen levels were assessed in washed cell lysates. A representative immunoblot showing fibrinogen and RUNX1 is shown with quantification on the right (n = 4 experiments). (D) Fibrinogen levels over 24 hours in HEL cells treated with control or *RUNX1* siRNAs and monitored in buffer without fibrinogen. HEL cells treated with *RUNX1* or control siRNAs were washed and resuspended in media with added 10% FBS and 50 μg/mL fibrinogen for 24 hours at 37°C. Cells were washed, resuspended in media without fibrinogen or FBS. Fibrinogen levels were assessed in lysates by immunoblotting at time points shown. Shown is a representative immunoblot and quantification from 4 separate experiments.

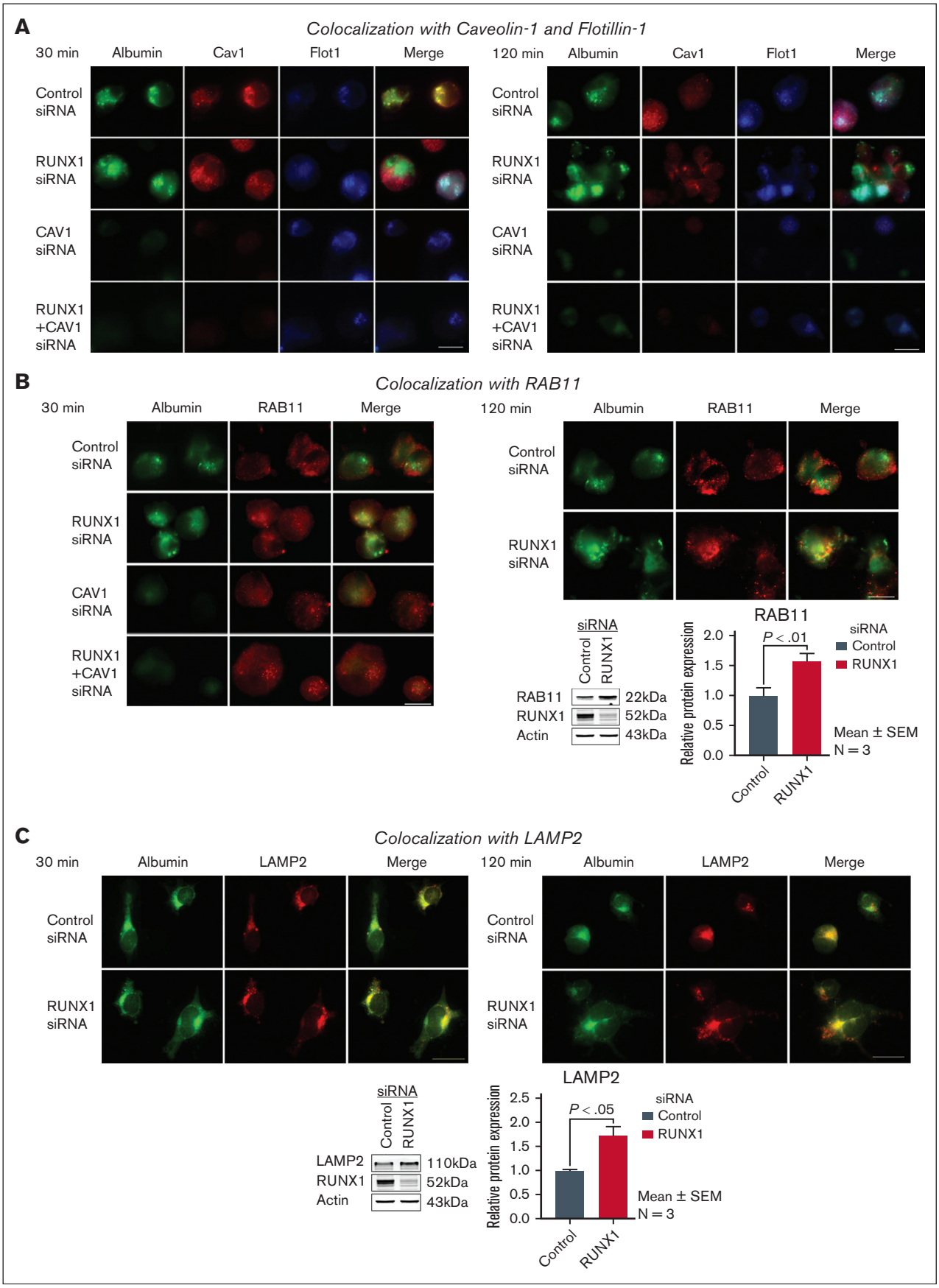

Figure 4.

endocytosis is defective in our patients (Figure 1), constituting 1 explanation. In addition, we provide evidence that *RUNX1*-deficient HEL cells and primary MK have increased endocytosis but defective trafficking of albumin and fibrinogen, by distinct mechanisms, leading to decreased levels. Multiple pathways drive endocytosis, mediated by clathrin, Cav1, and Flot1, and others.[2-4,40] Cav1 and Flot1, but not clathrin, were increased in *RUNX1*-deficient HEL cells (Figure 2B) and MK (Figure 7C). *CAV1* KD nearly eliminated intracellular albumin (Figure 4) and the increase in albumin uptake with *RUNX1* KD (Figure 2), indicating that Cav1 regulates albumin uptake, as shown in renal podocytes.[32] *CAV1* KD did not reduce intracellular fibrinogen (Figure 5), and *CAV1* KD did not abrogate the increased fibrinogen uptake on *RUNX1* KD (Figure 3), indicating that distinct mechanisms mediate albumin and fibrinogen endocytosis. Flot1 may have a role in fibrinogen handling, suggested by partial inhibition noted on *FLOT1* KD in *RUNX1*-deficient cells (Figure 3B). MK from induced-pluripotent stem cells from a patient with FPDMM had increased uptake of factor V,[41] a protein not synthesized by human MK. Thus, endocytosis of multiple proteins is increased in RHD. Interestingly, in *NBEAL2*-null mouse (gray platelet syndrome) MK fibrinogen uptake was normal but associated with defective retention,[42] indicating differences from RHD.

MK fibrinogen uptake is αIIbβ3 receptor-mediated[1,35,39] and clathrin- and ARF6- dependent.[1,35] In RUNX1-deficient HEL cells, there was no increase in surface αIIbβ3 (Figure 6), clathrin, or ARF6 (Figure 2D). Studies in sepsis advance IFITM3 as a regulator of platelet or MK fibrinogen endocytosis.[39] IFITM3 was upregulated in *RUNX1*-deficient HEL cells and primary MK (Figures 6E and 7C), but *IFITM3* KD did not inhibit fibrinogen uptake (supplemental Figure 2), suggesting that in these cells it may not be IFITM3-driven. IFITM3 effect in sepsis[39] may require other interferon-induced genes as well.[43,44]

Our studies suggest that *RUNX1* deficiency alters intracellular trafficking of albumin and fibrinogen and in a differential manner. On *RUNX1* KD, there was a decrease in albumin colocalization with Cav1 and an increase with Flot1 (Figure 4). Cav1 and Flot1 are distinct clathrin-independent mechanisms of endocytosis,[2,45] and they do not colocalize.[2] The cargo of Flot1-positive endosomes has been shown to be delivered to lysosomes[46,47] with Flot1 present on cytosolic face of lysosomes.[48,49] Lysosomal marker LAMP2 was increased on *RUNX1* downregulation, and albumin colocalized with LAMP2 (Figures 4 and 7). Albumin has been reported to traffic to lysosomes in which it is degraded.[32,37] Thus, albumin mistrafficking with lysosomal degradation is a mechanism in RHD-MK with decreasing levels over time and in platelet progeny.

In MK, after endocytosis, fibrinogen sequentially traffics from early endosomes to multivesicular bodies to late endosomes, and then to α-granules or recycling endosomes.[42] We show that fibrinogen trafficking is perturbed in *RUNX1*-deficient cells. RAB11 was upregulated (Figure 4B) and fibrinogen colocalized with RAB11 (Figure 5B), involved in protein recycling at plasma membrane,[27,50] and cell fibrinogen was decreased (Figure 3C). We postulate that there is enhanced fibrinogen recycling in RHD-MK, as described in *NBEAL2*$^{-/-}$ MK,[6] although lysosomal degradation is not excluded. Thus, the released platelets in RHD have lower fibrinogen plus impaired uptake.

Our studies in primary MK support remarkably well the findings in HEL cells with respect to the changes with RHD-increased uptake of albumin and fibrinogen, upregulation of several involved proteins and some aspects of mistrafficking (Figure 7). Additional studies are needed in MK to delineate these mechanisms.

The overall model (see visual abstract) that emerges is that RUNX1-deficient MK have enhanced endocytosis of albumin and fibrinogen but is associated with defective trafficking and loss of protein via lysosomal degradation or recycling, leading to decreased levels in MK, despite the enhanced endocytosis, and subsequently in platelet progeny. In addition, patient platelets had impaired endocytosis. Studies in a larger number of patients are needed to establish this and the involved proteins or genes. The impaired trafficking is likely related to aberrant granule formation and driven by dysregulation of numerous RUNX1-regulated genes and secondary somatic gene alterations.[18,29,51] We have shown that RUNX1-regulated GTPases, *RAB1B*,[24] and *RAB31*,[23] are decreased in RHD platelets and MK with altered endosomal trafficking of VWF, mannose 6-phosphate receptor, epidermal growth factor receptor, and strikingly enlarged early-endosomes.[23] These likely contribute to the protein mistrafficking.

IFITMs are important effectors in innate immunity and cancer biology,[43,44] and RUNX1 negatively regulates neutrophil cytokine production.[52,53] IFITM3 upregulation in *RUNX1*-deficient MK (Figures 6 and 7) is novel and maybe relevant to autoimmune manifestations[12,54] and leukemic predisposition of FPDMM. RUNX1 may negatively regulate *IFITM3*; platelet *IFITM3*

Figure 4. Effect of siRNA KD of RUNX1, CAV1, or both on albumin colocalization with Cav1, Flot1, RAB11, and LAMP2 in HEL cells by immunofluorescence microscopy. (A) Representative images showing the effect of KD of *RUNX1* or *CAV1* alone or in combination on albumin colocalization with Cav1 and Flot1. Control cells and those with siRNA KD of *RUNX1*, *CAV1*, or the combination were incubated with 30 μg/mL albumin Alexa 488 for 30 and 120 minutes, fixed and immobilized on poly-L-lysine-coated coverslips. Albumin is shown in green fluorescence. HEL cells were additionally stained with anti-Cav1 (red) or anti- Flot1 (blue) antibodies to assess colocalization as seen in merged images, evaluated by Epifluorescence microscope (EVOS FL Autoimaging). Because HEL cells had minimal endogenous Cav1, it was enhanced to assess colocalization with albumin. At 30 minutes, in control cells albumin (green) was colocalized with Cav1 (red), as shown in yellow in merged images, but not with Flot1 (blue). With *RUNX1* KD, albumin colocalization with Cav1 was decreased with increased colocalization with Flot1. With *CAV1* KD alone no albumin was discernible. At 120 minutes, with *RUNX1* KD there was a decrease in albumin colocalization with Cav1 and an increase with Flot1. (B) Representative images showing the effect of KD of *RUNX1* or *CAV1* alone or in combination on albumin (green) colocalization with RAB11 (red), a marker for recycling endosomes. At 30 or 120 minutes, there was low colocalization of albumin (green) with RAB11 (red) in control cells or on *RUNX1* KD. On *CAV1* KD alone or together with *RUNX1* KD there was negligible albumin in the cells. Representative immunoblots showing RAB11, RUNX1, and actin levels and densitometric quantification are shown. Data are shown as mean ± SEM (n = 4). (C) Representative images showing the effect of KD of *RUNX1* or *CAV1* alone or in combination on albumin (green) colocalization with lysosomal marker LAMP2 (red). At 30 minutes, there was some colocalization of albumin with LAMP2 in control cells and on *RUNX1* KD. At 120 min the colocalization of albumin with LAMP2 appeared more prominent with *RUNX1* KD than in control cells. Representative immunoblot showing protein expression of LAMP2, *RUNX1*, and actin, and densitometric quantification. Shown as mean ± SEM (n = 3).

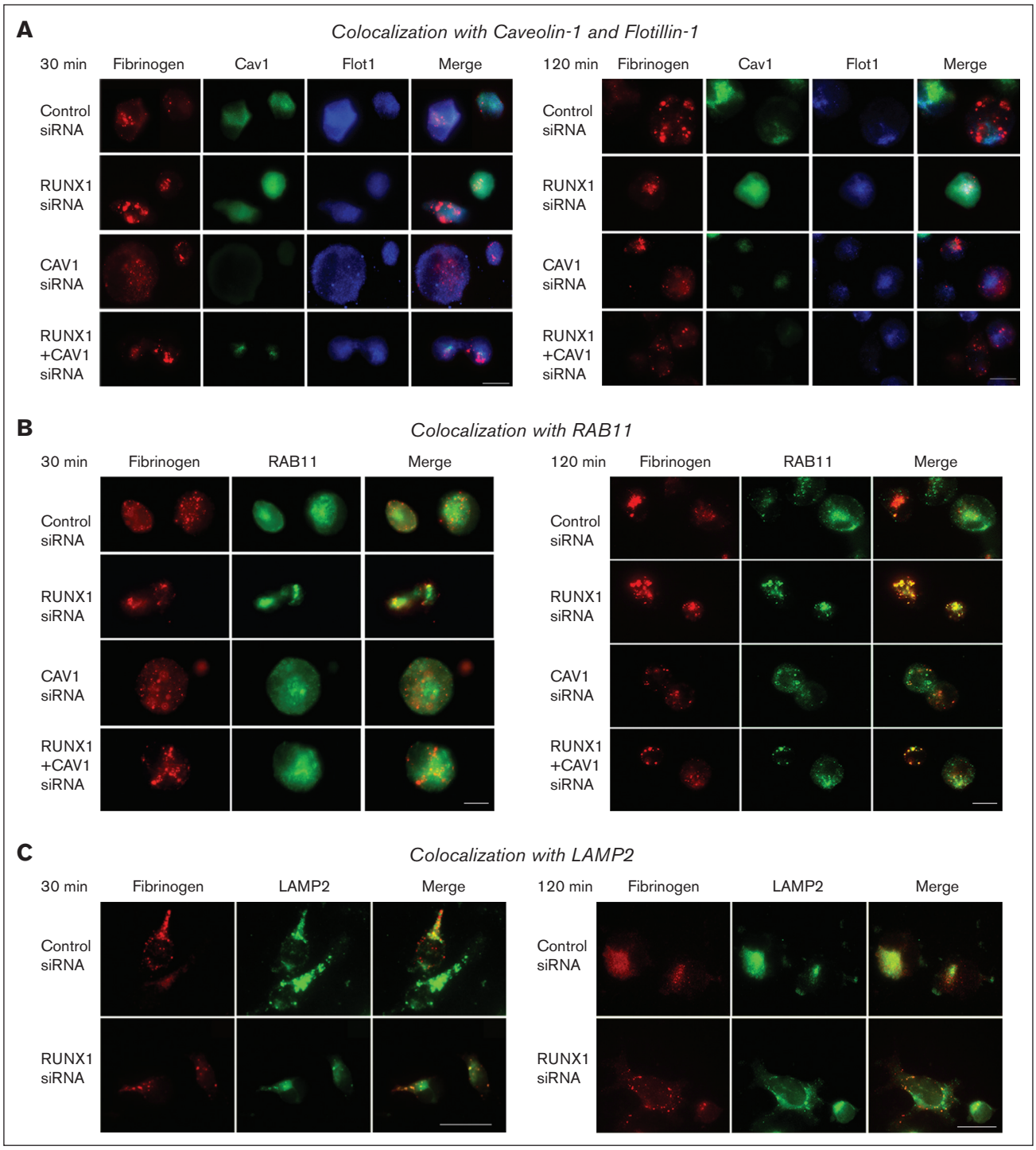

Figure 5. Effect of siRNA KD of RUNX1, CAV1, or both on fibrinogen colocalization with Cav1, Flot1, RAB11, and LAMP2 in HEL cells by immunofluorescence microscopy. (A) Representative images showing the effect of KD of *RUNX1* or *CAV1* alone or in combination on fibrinogen colocalization with Cav1 and Flot1. The experimental design was same as in Figure 4. HEL-cell suspensions (control cells and those with siRNA KD of *RUNX1*, *CAV1*, or combination) were incubated with fibrinogen Alexa 647, fixed, and immobilized on poly-lysine-coated coverslips. HEL cells were additionally stained with anti-Cav1 (green) or anti-Flot1 (blue) antibodies to assess colocalization as seen in merged images, evaluated by Epifluorescence microscope (EVOS FL Autoimaging). Because HEL cells had minimal endogenous Cav1, it was enhanced to assess colocalization with albumin. At 30 and 120 minutes, in control cells fibrinogen (red) showed no colocalization with Cav1 (green) or with Flot1 (blue). With *CAV1* KD alone fibrinogen uptake was unaffected compared to control cells. (B) Representative images showing the effect of KD of *RUNX1*, *CAV1* KD, or the combination on fibrinogen (red) colocalization with RAB11 (green), a marker for recycling endosomes. At 30 minutes, there was low to moderate fibrinogen colocalization (merged images, yellow) with RAB11 in control cells, and this was increased with *RUNX1* KD and with KD of *RUNX1+CAV1* (left panel); the colocalization with RAB11 was more prominent at 120 minutes (right panel). (C) Representative images showing the effect of KD of *RUNX1* or *CAV1* KD alone or in combination on colocalization of fibrinogen with lysosomal marker LAMP2 (green). At 30 (left panel) or 120 (right panel) minutes, there was similar low colocalization of fibrinogen (red) with LAMP2 (green) in control cells or on *RUNX1* KD.

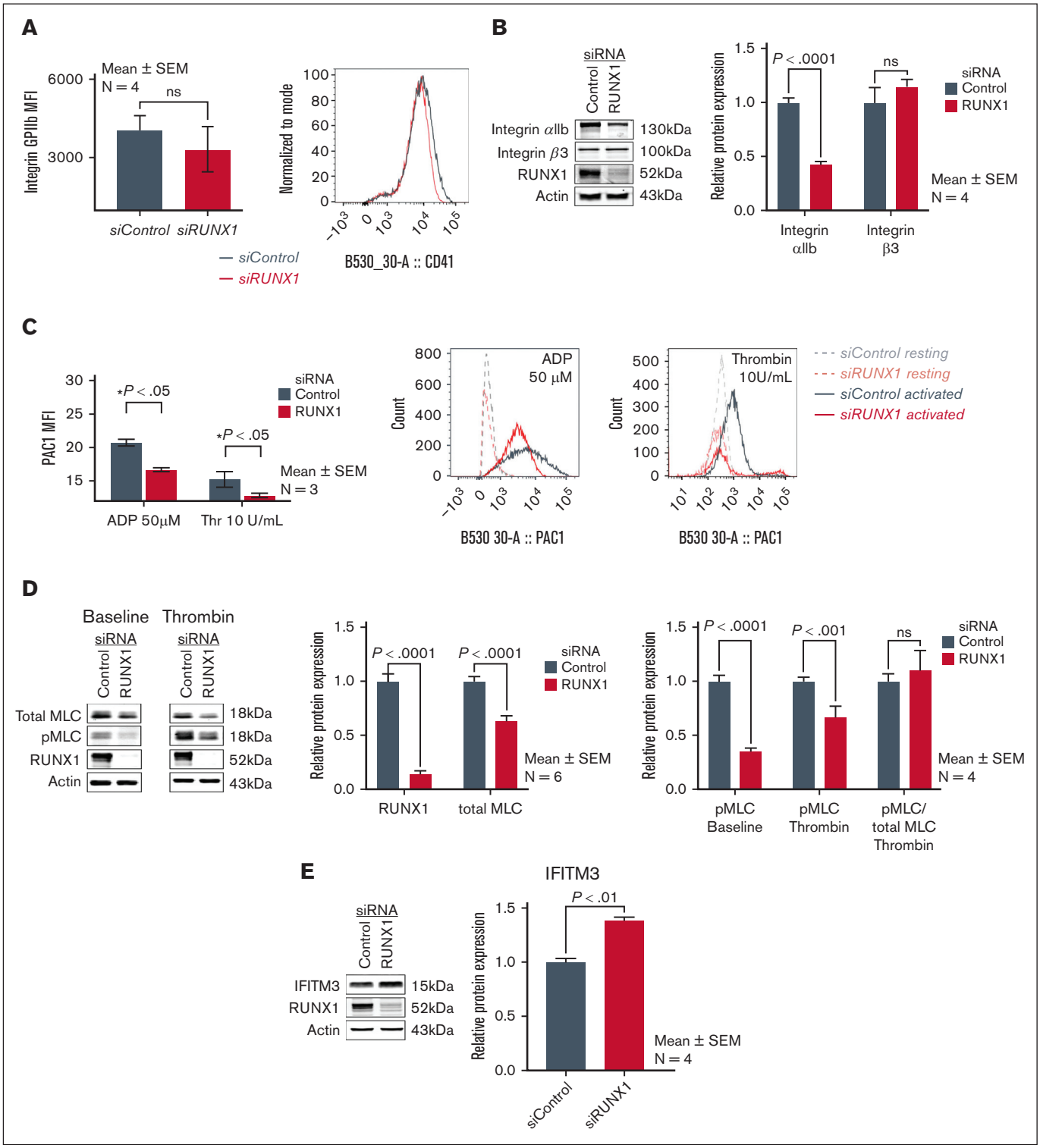

Figure 6. Effect of *RUNX1* KD on αIIbβ3 expression and activation, MLC expression and phosphorylation, and IFITM3 in HEL cells. (A) Effect of *RUNX1* KD on αIIbβ3 expression in HEL cells by flow cytometry using anti-CD41a antibody. (B) Representative immunoblots of αIIb, β3, RUNX1, and β-actin protein expression and densitometric quantification (n = 4). *P* values show comparisons by the Student *t* test. (C) Effect of *RUNX1* KD on αIIbβ3 activation evaluated by flow cytometry. FITC-labeled PAC1 antibody was used to assess activation of αIIbβ3 complex in control HEL cells (black lines) and after *RUNX1* KD (red lines), in the resting state (interrupted lines) and upon stimulation with ADP (50 μM) or thrombin (10 U/mL) (continuous lines). Data are expressed in arbitrary units as mean ± SEM (n = 3). (D) Effect of *RUNX1* KD on MLC expression and its phosphorylation upon thrombin activation in HEL cells. Left panel: representative immunoblots of total MLC, phospho-MLC (pMLC), RUNX1, and actin protein expression in control cells and those with *RUNX1* KD, in the resting state (baseline) and after thrombin activation (5 U/mL). Right panel: relative protein expression of RUNX1 and total MLC, and of pMLC in resting state (baseline) and after thrombin (5 U/mL) activation in control and *RUNX1*-deficient cells. The last 2 bars show the pMLC as a fraction of the total MLC present in control cells and *RUNX1* deficient cells. (E) Representative immunoblots showing relative protein expression in HEL cells of IFITM3, *RUNX1*, and actin, and densitometric quantification on *RUNX1* KD. Data are shown as mean ± SEM (n = 4).

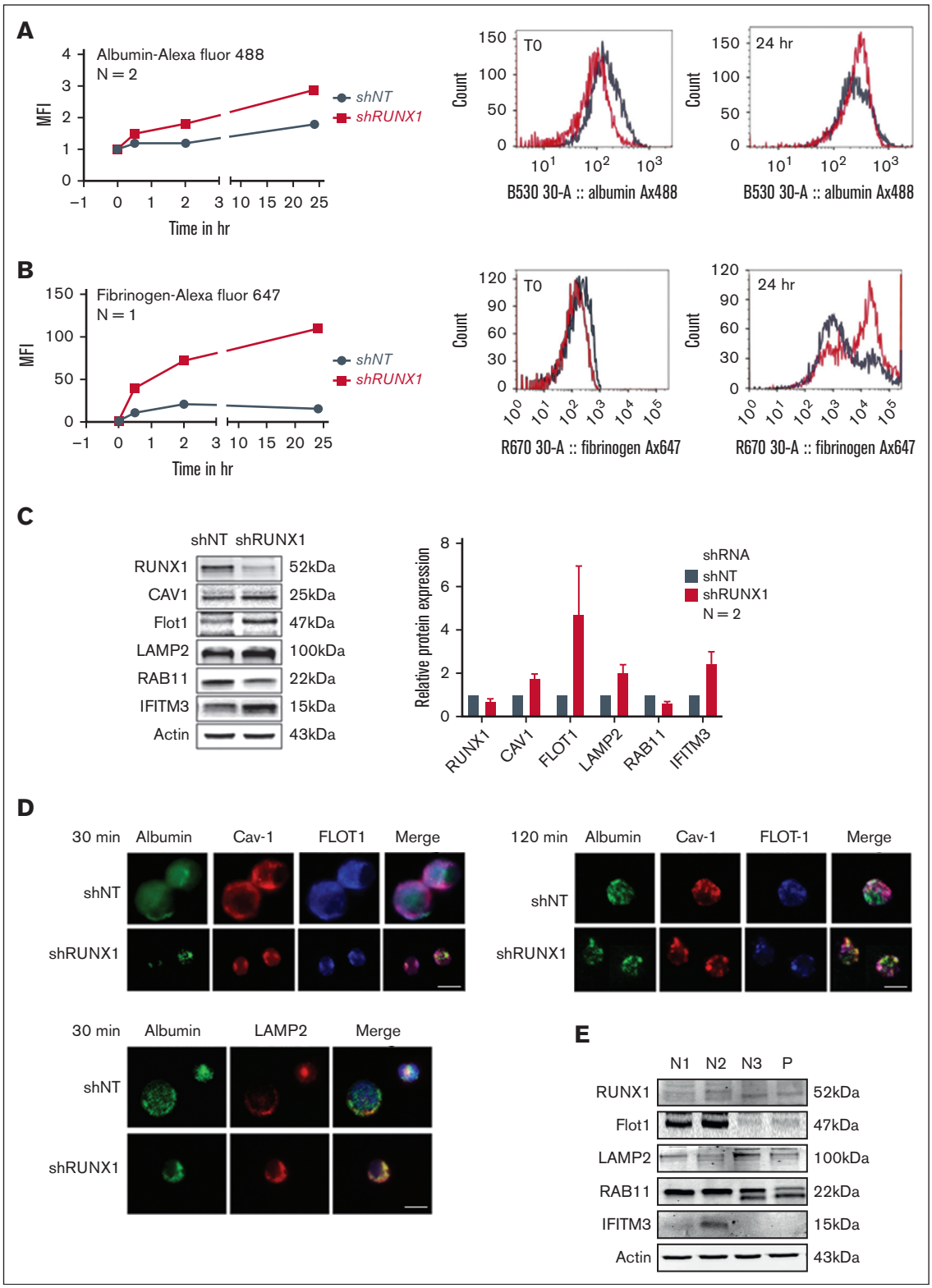

Figure 7. Effect of shRNA *RUNX1* KD in primary human MK on albumin and fibrinogen uptake and platelet levels of Flot1, LAMP2, RAB11, and IFITM3 in patient with FPDMM. (A) Effect of shRNA *RUNX1* KD in primary MK on uptake of albumin by flow cytometry. MK were differentiated in vitro from human CD34$^+$ cells for 12 days. CD34$^+$ cells were infected with sh*RX1*- or shNT-lentiviruses and expressing mCherry (mCherry$^+$) and sorted on day 4 of differentiation. From day 5 cells were cultured until day 11 or day 12 to mature MK and used for protein uptake studies using flow cytometry as described for HEL cells. Left panel: line graph shows MFI of albumin Alexa 488 uptake by MK overtime. Black lines indicate shNT and red shRX MK. Shown mean of 2 experiments. Right panel: representative histograms of albumin Alexa 488 uptake at the initial time point and 24 hours. (B) Effect of shRNA *RUNX1* KD in MK on uptake of fibrinogen Alexa 647 by flow cytometry. Black lines indicate shNT and red shRX MK. (C) Effect of shRNA *RUNX1* KD in MK on

messenger RNA is elevated in FPDMM.[51] IFITM3 is implicated in the pathogenesis of malignancies,[43,44,55,56] and acute myeloid leukemia patients with high expression have worse prognosis.[57]

Our studies advance the complex mechanistic basis of the FPDMM abnormalities in α-granules and their cargoes. These include dysregulated endocytosis and vesicular trafficking, poorly understood in platelet and MK but shared cellular processes potentially relevant to FPDMM manifestations beyond defective hemostasis.

Acknowledgments

The authors are grateful to the patients who have supported our studies over many years. The authors thank David E. Ambrose and Amir Yarmahmoodi for discussions and assistance in the flow cytometry studies.

This study was supported by research fundings from National Institutes of Health National Heart, Lung, and Blood Institute (grants R01 HL137376 and R01 HL109568 to A.K.R.; grants R01 HL137207 and HL159006 to L.E.G.; and grant R35 HL150698 to M.P.), the American Heart Association Transformational Project Award (grant 20TPA35490278) to L.E.G., and a RUNX1 Research Program/Alex's Lemonade Foundation grant to M.P.

Authorship

Contribution: F.D.C.-C., G.M., and L.G. performed the research, analyzed the data, and contributed to manuscript writing; J.W. performed the research and analyzed the data specifically for the immunofluorescence studies; A.M.A. performed the research; K.L. and M.P. generously provided the megakaryocytes differentiated from the human CD34$^+$ cells with RUNX1 knockdown and their expertise; A.K.R. and L.E.G. conceived and designed, performed the research, interpreted data, and wrote the manuscript; and all authors contributed to the manuscript, read, and approved the manuscript.

Conflict-of-interest disclosure: The authors declare no competing financial interests.

ORCID profiles: L.E.G., 0000-0003-0525-6008; L.G., 0000-0002-7470-564X; M.A.A., 0000-0001-5801-2512; K.L., 0000-0003-1340-3602; M.P., 0000-0001-7237-3613; A.K.R., 0000-0002-3078-7778.

Correspondence: A. Koneti Rao, Sol Sherry Thrombosis Research Center and Section of Hematology, Lewis Katz School of Medicine at Temple University, 3420 N. Broad St, 204 MRB, Philadelphia, PA 19140; email: koneti@temple.edu.

References

1. Banerjee M, Whiteheart SW. The ins and outs of endocytic trafficking in platelet functions. *Curr Opin Hematol*. 2017;24(5):467-474.
2. Glebov OO, Bright NA, Nichols BJ. Flotillin-1 defines a clathrin-independent endocytic pathway in mammalian cells. *Nat Cell Biol*. 2006;8(1):46-54.
3. Parton RG. Caveolae: structure, function, and relationship to disease. *Annu Rev Cell Dev Biol*. 2018;34:111-136.
4. Rennick JJ, Johnston APR, Parton RG. Key principles and methods for studying the endocytosis of biological and nanoparticle therapeutics. *Nat Nanotechnol*. 2021;16(3):266-276.
5. Kaksonen M, Roux A. Mechanisms of clathrin-mediated endocytosis. *Nat Rev Mol Cell Biol*. 2018;19(5):313-326.
6. Kahr WH, Hinckley J, Li L, et al. Mutations in NBEAL2, encoding a BEACH protein, cause gray platelet syndrome. *Nat Genet*. 2011;43(8):738-740.
7. de Bruijn M, Dzierzak E. Runx transcription factors in the development and function of the definitive hematopoietic system. *Blood*. 2017;129(15):2061-2069.
8. de Bruijn MF, Speck NA. Core-binding factors in hematopoiesis and immune function. *Oncogene*. 2004;23(24):4238-4248.
9. Bonifer C, Levantini E, Kouskoff V, Lacaud G. Runx1 structure and function in blood cell development. *Adv Exp Med Biol*. 2017;962:65-81.
10. Song WJ, Sullivan MG, Legare RD, et al. Haploinsufficiency of CBFA2 causes familial thrombocytopenia with propensity to develop acute myelogenous leukaemia. *Nat Genet*. 1999;23(2):166-175.
11. Songdej N, Rao AK. Hematopoietic transcription factor mutations: important players in inherited platelet defects. *Blood*. 2017;129(21):2873-2881.
12. Brown AL, Arts P, Carmichael CL, et al. RUNX1-mutated families show phenotype heterogeneity and a somatic mutation profile unique to germline predisposed AML. *Blood Adv*. 2020;4(6):1131-1144.
13. Sood R, Kamikubo Y, Liu P. Role of RUNX1 in hematological malignancies. *Blood*. 2017;129(15):2070-2082.
14. Cunningham L, Merguerian M, Calvo KR, et al. Natural history study of patients with familial platelet disorder with associated myeloid malignancy. *Blood*. 2023;142(25):2146-2158.
15. Mao G, Songdej N, Voora D, et al. Transcription factor RUNX1 regulates platelet PCTP (phosphatidylcholine transfer protein): implications for cardiovascular events: differential effects of RUNX1 variants. *Circulation*. 2017;136(10):927-939.

Figure 7 (continued) levels of RUNX1, Cav1, Flot1, LAMP2, RAB11, IFITM3, and actin (as loading control) by immunoblotting. Shown on the right is the relative protein levels done in duplicate. (D) Effect of shRNA RUNX1 KD in MK on albumin colocalization with Cav1, and Flot1 (top panels, 30 and 120 minutes) and with LAMP2 (bottom panel, 30 minutes) by immunofluorescence microscopy. Representative images are shown. shNT and shRX cells were incubated with 30 μg/mL albumin Alexa 488 for 30 and 120 minutes, fixed and immobilized on poly-L-lysine-coated coverslips. Albumin is shown in green fluorescence. In the top panels, cells were additionally stained with anti-Cav1 (red) or anti-Flot1 (blue) antibodies to assess colocalization as seen in merged images. In the bottom panel the cells were additionally stained with anti-LAMP2 (blue). (E) Platelet levels of Flot1, LAMP2, RAB11 and IFITM3 in patient with FPDMM (P, father) and 3 healthy donors (N, 1-3).

16. Mao GF, Goldfinger LE, Fan DC, et al. Dysregulation of PLDN (pallidin) is a mechanism for platelet dense granule deficiency in RUNX1 haplodeficiency. *J Thromb Haemost*. 2017;15(4):792-801.
17. Gabbeta J, Yang X, Sun L, McLane MA, Niewiarowski S, Rao AK. Abnormal inside-out signal transduction-dependent activation of glycoprotein IIb-IIIa in a patient with impaired pleckstrin phosphorylation. *Blood*. 1996;87(4):1368-1376.
18. Sun L, Gorospe JR, Hoffman EP, Rao AK. Decreased platelet expression of myosin regulatory light chain polypeptide (MYL9) and other genes with platelet dysfunction and CBFA2/RUNX1 mutation: insights from platelet expression profiling. *J Thromb Haemost*. 2007;5(1):146-154.
19. Sun L, Mao G, Rao AK. Association of CBFA2 mutation with decreased platelet PKC-θ and impaired receptor-mediated activation of GPIIb-IIIa and pleckstrin phosphorylation: proteins regulated by CBFA2 play a role in GPIIb-IIIa activation. *Blood*. 2004;103(3):948-954.
20. Jalagadugula G, Mao G, Kaur G, Goldfinger LE, Dhanasekaran DN, Rao AK. Regulation of platelet myosin light chain (*MYL9*) by RUNX1: implications for thrombocytopenia and platelet dysfunction in *RUNX1* haplodeficiency. *Blood*. 2010;116(26):6037-6045.
21. Aneja K, Jalagadugula G, Mao G, Singh A, Rao AK. Mechanism of platelet factor 4 (PF4) deficiency with RUNX1 haplodeficiency: RUNX1 is a transcriptional regulator of *PF4*. *J Thromb Haemost*. 2011;9(2):383-391.
22. Jalagadugula G, Mao G, Kaur G, Dhanasekaran DN, Rao AK. Platelet protein kinase C-theta deficiency with human RUNX1 mutation: PRKCQ is a transcriptional target of RUNX1. *Arterioscler Thromb Vasc Biol*. 2011;31(4):921-927.
23. Jalagadugula G, Mao G, Goldfinger LE, et al. Defective RAB31-mediated megakaryocytic early endosomal trafficking of VWF, EGFR, and M6PR in RUNX1 deficiency. *Blood Adv*. 2022;6(17):5100-5112.
24. Jalagadugula G, Goldfinger LE, Mao G, Lambert MP, Rao AK. Defective RAB1B-related megakaryocytic ER-to-golgi transport in RUNX1 haplodeficiency: impact on von Willebrand factor. *Blood Adv*. 2018;2(7):797-806.
25. Parton RG, Collins BM. The structure of caveolin finally takes shape. *Sci Adv*. 2022;8(19):eabq6985.
26. Stenmark H. Rab GTPases as coordinators of vesicle traffic. *Nat Rev Mol Cell Biol*. 2009;10(8):513-525.
27. Takahashi S, Kubo K, Waguri S, et al. Rab11 regulates exocytosis of recycling vesicles at the plasma membrane. *J Cell Sci*. 2012;125(pt 17):4049-4057.
28. Jalagadugula G, Dhanasekaran DN, Kim S, Kunapuli SP, Rao AK. Early growth response transcription factor EGR-1 regulates Galphaq gene in megakaryocytic cells. *J Thromb Haemost*. 2006;4(12):2678-2686.
29. Estevez B, Borst S, Jarocha D, et al. RUNX-1 haploinsufficiency causes a marked deficiency of megakaryocyte-biased hematopoietic progenitor cells. *Blood*. 2021;137(19):2662-2675.
30. Lee K, Ahn HS, Estevez B, Poncz M. RUNX1-deficient human megakaryocytes demonstrate thrombopoietic and platelet half-life and functional defects. *Blood*. 2023;141(3):260-270.
31. Schneider CA, Rasband WS, Eliceiri KW. NIH Image to ImageJ: 25 years of image analysis. *Nat Methods*. 2012;9(7):671-675.
32. Dobrinskikh E, Okamura K, Kopp JB, Doctor RB, Blaine J. Human podocytes perform polarized, caveolae-dependent albumin endocytosis. *Am J Physiol Renal Physiol*. 2014;306(9):F941-951.
33. Schubert W, Frank PG, Razani B, Park DS, Chow CW, Lisanti MP. Caveolae-deficient endothelial cells show defects in the uptake and transport of albumin in vivo. *J Biol Chem*. 2001;276(52):48619-48622.
34. Eaton N, Drew C, Wieser J, Munday AD, Falet H. Dynamin 2 is required for GPVI signaling and platelet hemostatic function in mice. *Haematologica*. 2020;105(5):1414-1423.
35. Huang Y, Joshi S, Xiang B, et al. Arf6 controls platelet spreading and clot retraction via integrin αIIbβ3 trafficking. *Blood*. 2016;127(11):1459-1467.
36. Carson JM, Okamura K, Wakashin H, et al. Podocytes degrade endocytosed albumin primarily in lysosomes. *PLoS One*. 2014;9(6):e99771.
37. Gekle M. Renal tubule albumin transport. *Annu Rev Physiol*. 2005;67:573-594.
38. Handagama P, Scarborough RM, Shuman MA, Bainton DF. Endocytosis of fibrinogen into megakaryocyte and platelet alpha-granules is mediated by alpha IIb beta 3 (glycoprotein IIb-IIIa). *Blood*. 1993;82(1):135-138.
39. Campbell RA, Manne BK, Banerjee M, et al. IFITM3 regulates fibrinogen endocytosis and platelet reactivity in nonviral sepsis. *J Clin Invest*. 2022;132(23):e153014.
40. Doherty GJ, McMahon HT. Mechanisms of endocytosis. *Annu Rev Biochem*. 2009;78:857-902.
41. Borst S, Nations CC, Klein JG, et al. Study of inherited thrombocytopenia resulting from mutations in ETV6 or RUNX1 using a human pluripotent stem cell model. *Stem Cell Rep*. 2021;16(6):1458-1467.
42. Lo RW, Li L, Leung R, Pluthero FG, Kahr WHA. NBEAL2 (neurobeachin-like 2) is required for retention of cargo proteins by alpha-granules during their production by megakaryocytes. *Arterioscler Thromb Vasc Biol*. 2018;38(10):2435-2447.
43. Friedlova N, Zavadil Kokas F, Hupp TR, Vojtesek B, Nekulova M. IFITM protein regulation and functions: far beyond the fight against viruses. *Front Immunol*. 2022;13:1042368.
44. Gomez-Herranz M, Taylor J, Sloan RD. IFITM proteins: understanding their diverse roles in viral infection, cancer, and immunity. *J Biol Chem*. 2023;299(1):102741.
45. Singh J, Elhabashy H, Muthukottiappan P, et al. Cross-linking of the endolysosomal system reveals potential flotillin structures and cargo. *Nat Commun*. 2022;13(1):6212.

46. Fan W, Guo J, Gao B, et al. Flotillin-mediated endocytosis and ALIX-syntenin-1-mediated exocytosis protect the cell membrane from damage caused by necroptosis. *Sci Signal*. 2019;12(583):eaaw3423.

47. Stuermer CA, Lang DM, Kirsch F, Wiechers M, Deininger SO, Plattner H. Glycosylphosphatidyl inositol-anchored proteins and fyn kinase assemble in noncaveolar plasma membrane microdomains defined by reggie-1 and -2. *Mol Biol Cell*. 2001;12(10):3031-3045.

48. Kaushik S, Massey AC, Cuervo AM. Lysosome membrane lipid microdomains: novel regulators of chaperone-mediated autophagy. *EMBO J*. 2006; 25(17):3921-3933.

49. Kokubo H, Helms JB, Ohno-Iwashita Y, Shimada Y, Horikoshi Y, Yamaguchi H. Ultrastructural localization of flotillin-1 to cholesterol-rich membrane microdomains, rafts, in rat brain tissue. *Brain Res*. 2003;965(1-2):83-90.

50. Savina A, Vidal M, Colombo MI. The exosome pathway in K562 cells is regulated by Rab11. *J Cell Sci*. 2002;115(Pt 12):2505-2515.

51. Palma-Barqueros V, Bastida JM, Lopez Andreo MJ, et al. Platelet transcriptome analysis in patients with germline RUNX1 mutations. *J Thromb Haemost*. 2023;21(5):1352-1365.

52. Bellissimo DC, Chen CH, Zhu Q, et al. Runx1 negatively regulates inflammatory cytokine production by neutrophils in response to Toll-like receptor signaling. *Blood Adv*. 2020;4(6):1145-1158.

53. Zezulin AU, Yen D, Ye D, et al. RUNX1 is required in granulocyte-monocyte progenitors to attenuate inflammatory cytokine production by neutrophils. *bioRxiv*. 2023;37(13-14):605-620.

54. Sorrell A, Espenschied C, Wang W, et al. Hereditary leukemia due to rare RUNX1c splice variant (L472X) presents with eczematous phenotype. *Int J Clin Med*. 2012;03(07):607-613.

55. Rajapaksa US, Jin C, Dong T. Malignancy and IFITM3: friend or foe? *Front Oncol*. 2020;10:593245.

56. Lee J. Does IFITM3 link inflammation to tumorigenesis? *BMB Rep*. 2022;55(12):602-608.

57. Liu Y, Lu R, Cui W, et al. High IFITM3 expression predicts adverse prognosis in acute myeloid leukemia. *Cancer Gene Ther*. 2020;27(1-2):38-44.